

Photocatalytic Self-cleaning by Nanocomposite Fibers Containing Titanium Dioxide Nanoparticles

Taeyoung Jeong and Seungsin Lee*

Department of Clothing and Textiles, Yonsei University, Seoul 03722, Korea
(Received July 25, 2018; Revised October 2, 2018; Accepted October 7, 2018)

Abstract: Titanium dioxide (TiO₂), a well-known photocatalyst, was incorporated into poly(vinyl alcohol) (PVA) nanofibers via electrospinning to develop self-cleaning textile materials that can decompose organic contaminants and stains on the textile surface by light irradiation. TiO₂/PVA nanocomposite fiber webs were prepared from PVA solutions that contained 5, 10, and 20 wt% TiO₂ nanoparticles. The morphologies and chemical compositions of the composite fibers were characterized using scanning electron microscopy, transmission electron microscopy, and an energy dispersive X-ray analysis system. The TiO₂/PVA nanocomposite fiber webs were thermally treated to increase their stability in an aqueous environment. To evaluate the self-cleaning performance, the fiber webs were saturated using a methylene blue dye solution and red wine. Different light sources, *i.e.*, ultraviolet (UV) light, visible light, and fluorescent light, were used to examine their effects on the photocatalytic self-cleaning activities of the TiO₂/PVA nanocomposite fiber webs. The color changes of the methylene blue and red wine stains on the fiber webs were assessed with the time of light exposure over a period of 24 h. The results depicted that the decomposition rates of the methylene blue and red wine stains by the fiber webs varied in the order of fluorescent light < visible light < UV light. Generally, the decomposition rate increased by increasing the time of light exposure and the TiO₂ concentration. Our findings demonstrated the self-cleaning performance of the electrospun composite fibers containing TiO₂ nanoparticles not only under UV light but also under visible and fluorescent light that are commonly used indoors.

Keywords: Photocatalysis, Self-cleaning, Titanium dioxide, Nanocomposite fiber, Electrospinning

Introduction

Self-cleaning materials attract considerable attention due to economic, environmental, and aesthetic reasons. Such materials require low amount of labor for cleaning and no requirement of detergents, thereby reducing the cost of cleaning maintenance and resulting in minimal impact on the environment [1]. In the field of textiles, interest in self-cleaning fibrous materials has been increasing because of the extensive range of possible applications, including apparel fabrics, household textiles, and technical textiles.

Titanium dioxide (TiO₂), which is one of the most widely used photocatalysts, possesses diverse properties, such as disinfection, self-cleaning, and pollutant-decomposing properties, under sunlight or fluorescent light [2-4]. The photocatalytic process includes chemical steps that result in the generation of highly reactive species. The photocatalytic activity is initiated upon irradiation using light having an energy that is equal to or greater than the band gap energy of the photocatalyst [2]. The activated photocatalysts produce electron-hole pairs in which the excited electrons (e⁻) and the positive holes (h⁺) are formed in the conduction band and the valence band, respectively. These photogenerated electrons and holes produce oxygen and hydroxyl radicals that react with the adsorbed substances on the photocatalyst surface, which causes the decomposition of organic contaminants and microorganisms into carbon dioxide and water [1,5]. The crystal structure and particle size of TiO₂ are important factors to determine the photocatalytic activity [2,6]. Anatase

and rutile are observed to be common crystal structures among the three crystalline forms, *i.e.*, anatase, brookite, and rutile. Anatase has been reported to be more photoactive than rutile [1,7]. TiO₂ exhibits various advantages over other photocatalysts, *i.e.*, it exhibits chemical stability, low toxicity, relatively low production cost, and strong oxidizing ability [2,8]. Thus, TiO₂ has been extensively studied as a photocatalyst for air and water purification systems, disinfection, and self-cleaning building materials [2,8,9].

TiO₂ particles have been incorporated in fibrous materials using various methods, including a conventional pad-dry-cure process [10,11], dip coating with pretreated textiles such as plasma and ultraviolet (UV) irradiation [12,13], chemical spacers [14], or liquid phase deposition [15]. Although the coating of TiO₂ particles on the substrate surface exhibits considerable photocatalytic self-cleaning ability, variations in the fabric handle have been reported due to the presence of TiO₂ coating [16]. For some fibers, the attachment of TiO₂ on their surface is weak due to the lack of anchoring functional groups. Therefore, pretreatments, such as plasma and UV irradiation-induced surface activation, are proposed to improve the adhesion of TiO₂ with the substrates. However, they are expensive and difficult to implement on a large scale [3]. Thus, there is a requirement to develop novel approaches for the fabrication of self-cleaning fibrous materials.

Electrospinning is a relatively simple technique that produces fibers having ultrathin diameters [17,18]. Fibrous structures that comprise such thin fibers offer exceptionally large specific surface areas, which make them attractive for use in photocatalytic self-cleaning textile applications.

*Corresponding author: SL158@yonsei.ac.kr

Another advantage of electrospinning is that a desired functionality can be introduced to the ultrathin fibers via simultaneous spinning of the polymer material and a functional material in a single step [19]. Bedford and Steckl [20] prepared core-sheath nanofibers via co-axial electrospinning using cellulose acetate and nanocrystalline TiO₂ dispersion as the core and sheath, respectively. Such coaxial electrospun fibers were observed to exhibit outstanding photocatalytic self-cleaning effects. The high surface area-to-volume ratio of the nanofibrous structures played an important role during the photocatalytic activity. The co-axial electrospinning, however, requires a special apparatus, such as a coaxial dual-capillary spinneret, to which two polymer solutions are supplied using two separate syringe pumps and pipelines. To date, to the best of our knowledge, no research has investigated the self-cleaning effects of TiO₂ nanocomposite fibers prepared using an ordinary single-nozzle electrospinning setup. Thus, in this study, we address this deficiency to further explore the self-cleaning properties of TiO₂ nanocomposite fibers having different TiO₂ concentrations.

Light source is another important factor that affects the photocatalytic self-cleaning property. Because the UV component of the solar spectrum (200–400 nm) is observed to be responsible for the photocatalytic activity [20], evaluations of the photocatalytic self-cleaning effects are mainly implemented under UV irradiation. However, the photocatalytic self-cleaning properties should be assessed in light typical of an indoor working environment as well to examine the feasibility of the self-cleaning activity in an indoor environment for practical applications.

In this study, TiO₂/poly(vinyl alcohol) (PVA) nanocomposite fibers that contained various amounts of TiO₂ nanoparticles were prepared by electrospinning. The morphologies and chemical compositions of the nanocomposite fibers were characterized using field-emission scanning electron microscopy, transmission electron microscopy, and an energy dispersive X-ray analysis system. The PVA-based nanocomposite fiber webs were thermally treated to increase their stability in an aqueous environment. The self-cleaning performances of the fibers containing various amounts of TiO₂ nanoparticles were investigated by assessing the decomposition of the methylene blue and red wine stains under different light sources (UV lamps, visible lamps, and fluorescent lamps). Effects of the light sources and the TiO₂ concentration on the photocatalytic activities of the TiO₂ nanocomposite fibers

were examined with the time of light exposure over a period of 24 h.

Experimental

Materials

PVA (>99 % hydrolyzed, Mw=89,000–98,000, Sigma Aldrich Co., USA) was used as a polymer system. Distilled water was used as the solvent. Water-based nanosized colloidal TiO₂ (AERODISP[®] W740X, average diameter of 21 nm) was supplied by Degussa Co. (Germany). The crystal distribution of TiO₂ was 80 % anatase and 20 % rutile. Methylene blue (Fisher Scientific Inc., UK) and red wine (Carlo Rossi California Red, 11.5 % alc/vol) were used as the staining agents.

Electrospinning Process

PVA powders of 11 wt% were dissolved in distilled water at 80 °C and stirred using a magnetic stirrer for 6 h. Colloidal TiO₂ was further added to the PVA solutions and stirred for another 6 h to prepare the electrospinning solutions. The concentrations of TiO₂ in the solutions were set to 5, 10, and 20 wt% to examine the effect of TiO₂ concentration on the self-cleaning properties of the nanocomposite fibers.

Electrospinning was performed in a vertical electrospinning setup (NNC-ESP200R2, NanoNC Co., Korea). The system comprised a syringe with a needle, a high voltage power supply capable of delivering 0–30 kV, a syringe pump, and a grounded collector. As presented in Table 1, electrospinning was performed under different conditions to determine the suitable conditions for fabricating uniform nanocomposite fibers containing varied amounts of TiO₂ nanoparticles. The grounded collector was placed 13 cm from the needle tip. The TiO₂ nanocomposite fibers were electrospun and directly deposited onto a polyester woven substrate mounted on the grounded collector.

Fiber Morphology

The morphologies of the TiO₂ nanocomposite fibers were examined using a field-emission scanning electron microscope (FE-SEM; JSM-6701F, JEOL Ltd., Japan) after sputter-coating with Pt/Pd. A transmission electron microscope (TEM; JEM-2100F, JEOL Ltd., Japan) equipped with an energy dispersive X-ray (EDX) analysis system was used to further characterize the morphologies of the TiO₂ nanocomposite fibers and to examine their chemical compositions.

Table 1. Processing conditions for electrospinning the TiO₂/PVA solutions containing varied TiO₂ concentrations

Electrospinning condition	TiO ₂ concentration			
	0 wt%	5 wt%	10 wt%	20 wt%
Feed rate (m/h)	0.1, 0.2	0.1	0.1	0.1, 0.3, 0.5, 0.7, 1.0, 1.8, 2.0
Needle gauge	25, 26	25, 26	26, 27	22, 23, 24, 25, 26
Voltage (kV)	18, 19, 20	17, 18, 20	19, 20	16, 18, 20, 21, 22, 23, 25

To conduct the TEM examinations, the nanocomposite fibers were collected on a carbon-coated copper specimen grid.

Heat Treatment

The electrospun TiO₂/PVA nanocomposite fiber webs containing various amounts of TiO₂ nanoparticles were heat-treated at various temperatures ranging from 155 °C to 170 °C for different time periods (from 3 to 15 min) to determine the suitable heat treatment conditions. After heat treatment, both the heat-treated and untreated nanofiber webs were immersed in water at 18 °C for 1 h. The morphologies of the nanofiber webs were examined using the FE-SEM to verify the effect of heat treatment.

Assessment of the Photocatalytic Activities of TiO₂ Nanocomposite Fibers

The photocatalytic activities of the TiO₂ nanocomposite fibers were assessed by examining the color change of color stains on the fiber webs. The TiO₂/PVA nanocomposite fiber webs containing varied TiO₂ concentrations and pristine PVA nanofiber webs were prepared and cut into 7×14 cm pieces. The web area density of the electrospun fibrous webs was set as 3 g/m². The specimens were submerged in a 400-ml aqueous solution of methylene blue (0.1 g/l) and red wine for 30 min. These stained specimens were kept in dark and were dried in air without any light exposure for 24 h before exposing to light irradiation for 0, 1, 2, 3, 4, and 24 h. The experimental setup is depicted in Figure 1. Three different light sources, including the UV lamps (BLB lamp, λ_{max}=365 nm, Sankyo, Japan; 20 W×2 ea), visible lamps (TLD 15W/03 lamp, λ_{max}=420 nm, Philips, USA; 20 W×2 ea), and fluorescent lamps (Osram, Korea; 20 W×2 ea), were used to examine the effects of light sources on the photocatalytic activities of the TiO₂ nanocomposite fibers.

The color change over the duration of light exposure was evaluated using a spectrophotometer (SP-60, X-rite, USA). All the measurements were conducted in triplicate. The Kubelka-Munk equation (equation (1)) was used to define the relation between the reflectance of a sample and its

absorption and scattering characteristics:

$$K/S = \frac{(1-R)^2}{2R} \quad (1)$$

where, K is the absorption coefficient, S is the scattering coefficient of the sample, and R is the reflectance measured using a spectrophotometer.

The photocatalytic decomposition rates of the methylene blue and red wine stains were calculated using the following formula [21,22]:

$$\text{Decomposition (\%)} = \frac{(K/S)_S - (K/S)_L}{(K/S)_S - (K/S)_0} \times 100 \quad (2)$$

where, $(K/S)_S$, $(K/S)_L$, and $(K/S)_0$ denote the K/S values of the stained specimens before light exposure, after light exposure, and the non-stained specimens.

Results and Discussion

Fiber Morphology

We attempted to fabricate composite fibers containing varied amounts of TiO₂ nanoparticles to examine the effect of TiO₂ concentration on the self-cleaning properties of the TiO₂ nanocomposite fibers. The TiO₂/PVA solutions with TiO₂ concentrations of 5, 10, and 20 wt% were electrospun under various processing conditions, and the suitable spinning conditions for fabricating uniform nanocomposite fibers containing varied amounts of TiO₂ nanoparticles were determined. Figure 2 depicts the SEM micrographs of the pristine PVA fibers and composite fibers containing varied amounts of TiO₂ nanoparticles. Table 2 summarizes the spinning conditions used to fabricate the uniform TiO₂/PVA composite fibers containing varied amounts of TiO₂. The neat PVA nanofibers were produced from an 11 wt% PVA solution with a 26-gauge needle at a feed rate of 0.1 ml/h, a voltage of 20 kV, and a collecting distance of 13 cm. As depicted in Figure 2(a), cylindrical fibers having diameters of 180-280 nm were obtained. Figure 2(b) presents the SEM image of the nanocomposite fibers obtained from an 11 wt% PVA solution containing 5 wt% TiO₂. Bead-free composite

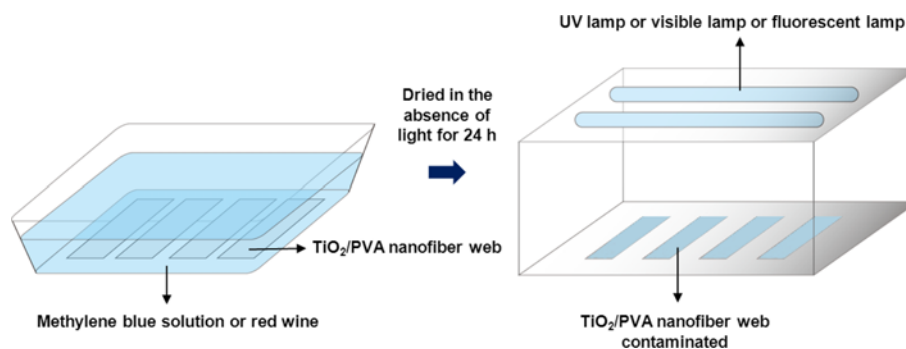


Figure 1. Experimental setup for the photocatalytic decomposition of the TiO₂/PVA nanocomposite fibers contaminated either by methylene blue or red wine.

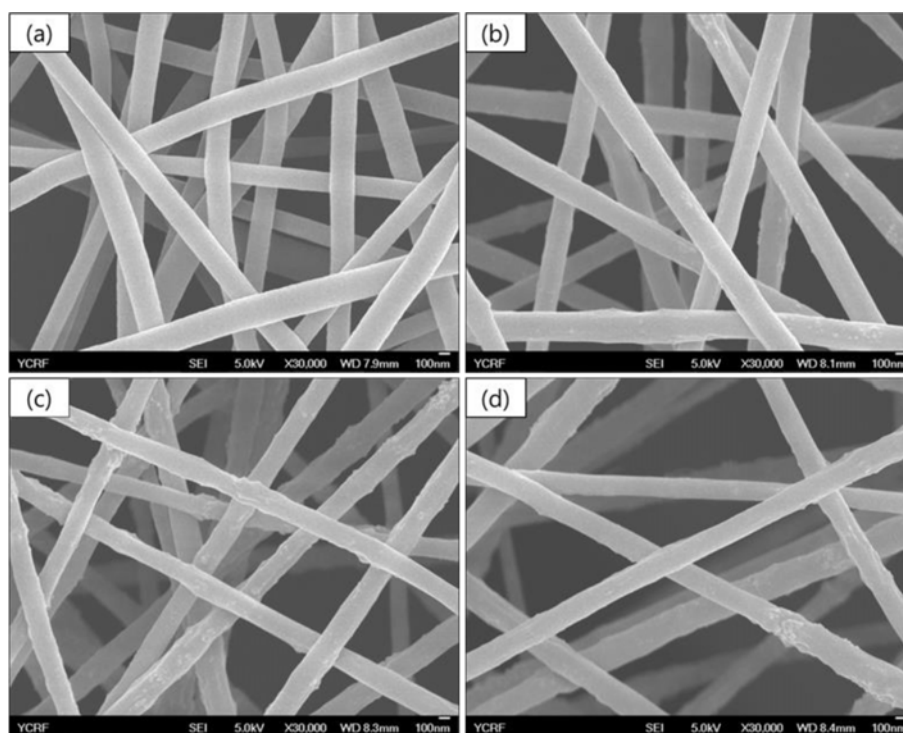


Figure 2. SEM images of the electrospun PVA and TiO_2 /PVA nanofibers: (a) PVA 11 wt%, 0.1 ml/h, 26 gauge, 20 kV, 13 cm, (b) TiO_2 5 wt%/PVA 11 wt%, 0.1 ml/h, 26 gauge, 20 kV, 13 cm, (c) TiO_2 10 wt%/PVA 11 wt%, 0.1 ml/h, 26 gauge, 20 kV, 13 cm, and (d) TiO_2 20 wt%/PVA 11 wt%, 2.0 ml/h, 25 gauge, 25 kV, 13 cm.

fibers were fabricated under a similar condition as that of the pristine PVA fibers and exhibited diameters of 200–250 nm. The final fibers (on a dry basis) contained 15 wt% TiO_2 and the remainder PVA. The composite fibers obtained from an 11 wt% PVA solution containing 10 wt% TiO_2 are depicted in Figure 2(c). The fibers were fabricated under similar spinning conditions to those fibers containing 15 wt% TiO_2 nanoparticles. In this case, the final fibers contained 27 wt% TiO_2 . Straight, bead-free composite fibers having diameters of 180–200 nm were obtained. The TiO_2 concentration in the spinning solution was further increased to 20 wt%. Figure 2(d) depicts the SEM image of the composite fibers obtained from an 11 wt% PVA solution containing 20 wt% TiO_2 . In this case, TiO_2 accounted for 42 wt% of the fiber mass. The fibers were fabricated using a 25-gauge needle at a feed rate of 2.0 ml/h, a voltage of 25 kV, and a collecting distance of 13 cm. These conditions yielded continuous, bead-free composite fibers having diameters of 180–210 nm. As depicted in Figures 2(b)–(d), the concentration of TiO_2 did not have a remarkable effect on the morphology of the resulting fibers. Thus, bead-free-shaped, uniform nanocomposite fibers were successfully fabricated from the TiO_2 /PVA solutions having TiO_2 concentrations of 5–20 wt%. Additionally, the spinning conditions that were suitable for fabricating uniform composite fibers were identified.

Table 2. Optimal electrospinning conditions for the TiO_2 /PVA solutions containing varied TiO_2 concentrations

Electrospinning condition	TiO_2 concentration			
	0 wt%	5 wt%	10 wt%	20 wt%
Feed rate (ml/h)	0.1	0.1	0.1	2.0
Needle gauge	26	26	26	25
Voltage (kV)	20	20	20	25
Distance (cm)	13	13	13	13

The TEM images and EDX spectra of the electrospun TiO_2 /PVA nanocomposite fibers containing varied amounts of TiO_2 nanoparticles are presented in Figures 3–5. As illustrated in the TEM images (Figures 3(a)–5(a)), TiO_2 nanoparticles were observed inside the composite fibers as well as on the surface of the fibers. The amount of TiO_2 nanoparticles in the composite fibers were observed to considerably increase as the TiO_2 concentration in the spinning solutions increased. The EDX analysis of the composite fibers indicates the presence of TiO_2 in these fibers, as depicted in Figures 3(b)–5(b). A considerable amount of Ti was detected in case of the composite fibers that were electrospun using the solutions having a high TiO_2 concentration.

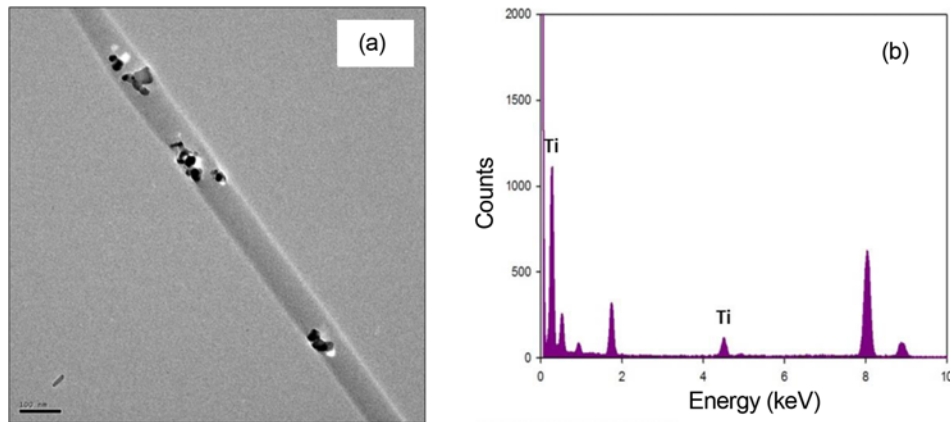


Figure 3. (a) TEM image and (b) EDX spectrum of the 15 wt% TiO₂/PVA nanofibers.

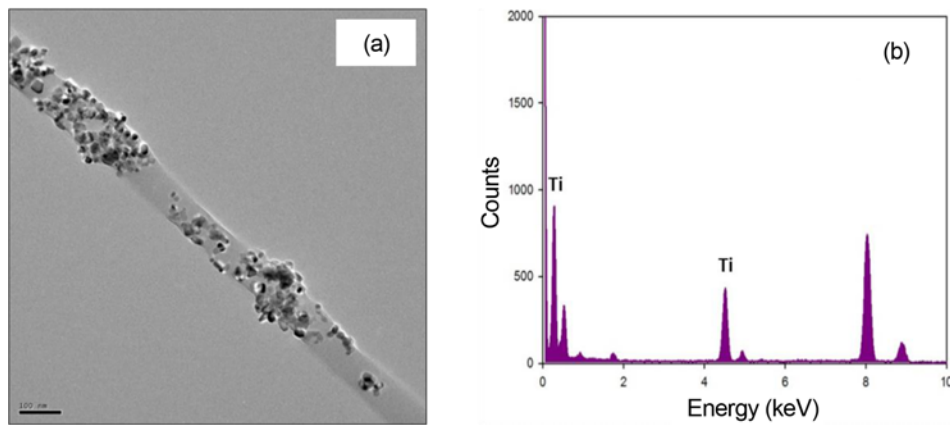


Figure 4. (a) TEM image and (b) EDX spectrum of the 27 wt% TiO₂/PVA nanofibers.

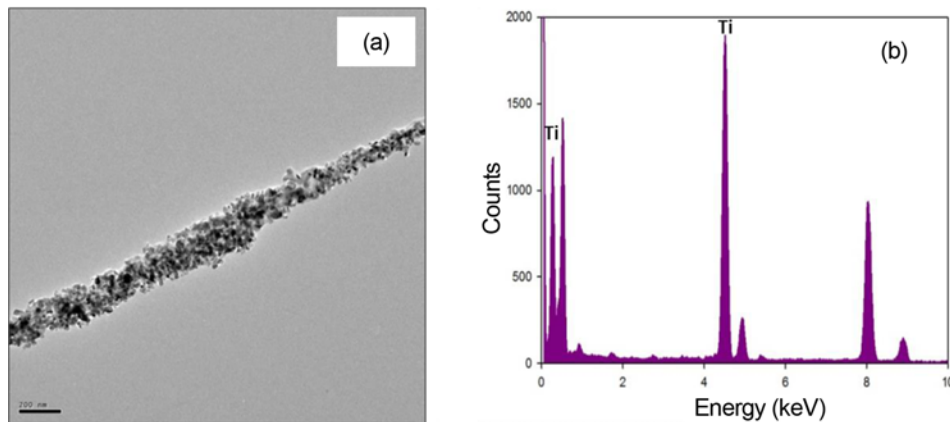


Figure 5. (a) TEM image and (b) EDX spectrum of the 42 wt% TiO₂/PVA nanofibers.

Effect of Heat Treatment

PVA nanofiber webs lose their nanofibrous structure when immersed in water; thus, heat treatment was performed to maintain the morphology and integrity of the PVA-based composite fibers. The electrospun TiO₂/PVA composite fiber webs containing varied amounts of TiO₂ nanoparticles were

thermally treated at various temperatures (from 155 °C to 170 °C) for different time periods (from 3 to 15 min) to determine the suitable heat treatment conditions.

Figure 6 depicts the morphologies of the nanofiber webs after immersing in water at 18 °C for 1 h. The as-spun PVA nanofibers were observed to completely lose their fibrous

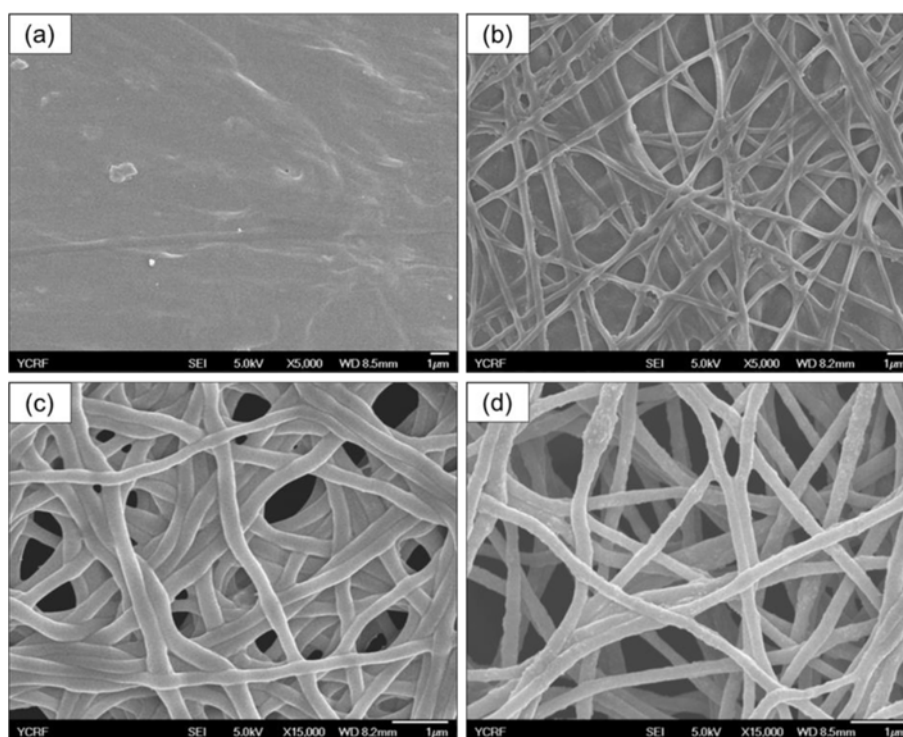


Figure 6. SEM images of the electrospun PVA and TiO_2/PVA nanofiber webs after being immersed in water: (a) PVA nanofibers without heat treatment, (b) PVA nanofibers after heat treatment at $160\text{ }^\circ\text{C}$ for 10 min, (c) 15 wt% TiO_2/PVA nanofibers after heat treatment at $165\text{ }^\circ\text{C}$ for 10 min, and (d) 27 wt% TiO_2/PVA nanofibers after heat treatment at $165\text{ }^\circ\text{C}$ for 15 min.

structure after exposure to an aqueous environment (Figure 6(a)). The heat treatment of the PVA nanofibers at $160\text{ }^\circ\text{C}$ for 10 min stabilized their fibrous structure (Figure 6(b)). Figure 6(c) depicts that the composite fibers containing 15 wt% TiO_2 nanoparticles maintained their fibrous structure after heat treatment at $165\text{ }^\circ\text{C}$ for 10 min. However, as the TiO_2 concentration was further increased to 27 and 42 wt%, the thermally treated composite fibers were partially dissolved in water. By increasing the heat treatment duration to 15 min, the composite fibers were observed to maintain their fibrous structure after being immersed in water. Figure 6(d) depicts that the composite fibers containing 27 wt% TiO_2 nanoparticles maintained their fibrous structure after heat treatment at $165\text{ }^\circ\text{C}$ for 15 min. Therefore, the suitable heat treatment conditions for the composite fibers containing 27 and 42 wt% TiO_2 nanoparticles were $165\text{ }^\circ\text{C}$ for 15 min. The TiO_2/PVA nanocomposite fiber webs containing varied amounts of TiO_2 nanoparticles attained stability in aqueous environments under different heat treatment conditions. The increase in the concentration of TiO_2 nanoparticles increased the required time of heat treatment for stabilizing the fiber morphology.

Photocatalytic Self-cleaning by TiO_2 Nanocomposite Fibers

The self-cleaning performance of the electrospun composite fibers containing varied amounts of TiO_2 nanoparticles were

investigated by assessing the decomposition of the methylene blue and red wine stains under different lighting conditions. Three different light sources, *i.e.*, UV lamps, visible lamps, and fluorescent lamps, were used to examine the effect of light sources on the photocatalytic activities of the TiO_2 nanocomposite fibers. Six irradiation durations of 0, 1, 2, 3, 4, and 24 h were employed to examine the color change with the time of light exposure.

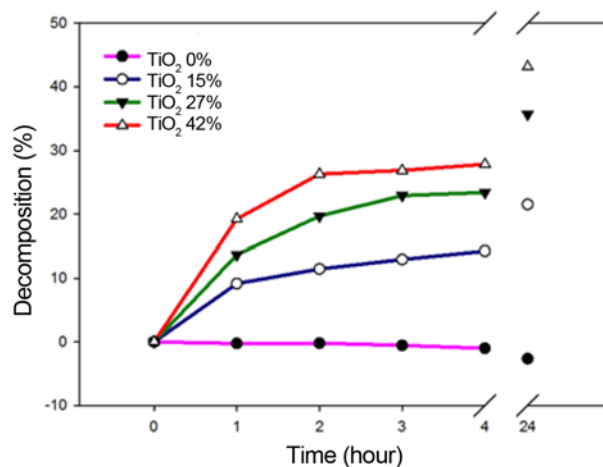


Figure 7. Degradation of the methylene blue stains on the TiO_2 nanocomposite fibers as a function of UV irradiation time.

Figure 7 depicts the degradation of methylene blue stains on the TiO₂ nanocomposite fibers as a function of the UV irradiation time. The nanocomposite fiber webs containing varied amounts of TiO₂ nanoparticles exhibited photocatalytic degradation activity, whereas pristine PVA fiber webs exhibited negligible degradation effect. The decomposition rate of the TiO₂-loaded nanofiber webs increased with the time of light exposure. Using the same duration of UV exposure, the fiber webs having high TiO₂ loading exhibited a high degradation rate. After UV irradiation for 24 h, the decomposition rates of methylene blue stains by the fiber webs containing 15, 27, and 42 wt% TiO₂ nanoparticles were 21.5 %, 35.7 %, and 43.1 %, respectively. The self-cleaning properties of TiO₂ are governed by the absorption of the band-gap light and the generation of electron-hole pairs [1]. The anatase-phase TiO₂ has been reported to be more photoactive than the rutile ones [1,7]. The band gap of anatase TiO₂ is 3.2 eV, which corresponds to the light having wavelength of 390 nm, *i.e.*, near-ultraviolet (UV) light [1]. Thus, we can expect that the TiO₂-loaded nanofibers will exhibit high photocatalytic activity under UV irradiation.

We further investigated the decomposition of the methylene blue stains under visible and fluorescent light to examine whether the photocatalytic self-cleaning activity of the fiber webs was feasible in indoor lighting conditions. Figures 8-10 present the decomposition rates of the methylene blue stains by the composite fiber webs containing 15, 27, and 42 wt% TiO₂ nanoparticles, respectively, under different light sources. The decomposition rates varied in the order of fluorescent light < visible light < UV light. Under the same light sources, the decomposition rate increased by increasing the TiO₂ loading. Although the best result was obtained under UV light, the TiO₂ composite fiber webs did exhibit photocatalytic self-cleaning characteristics under visible and fluorescent light. Fujishima and Zhang [2] reported that,

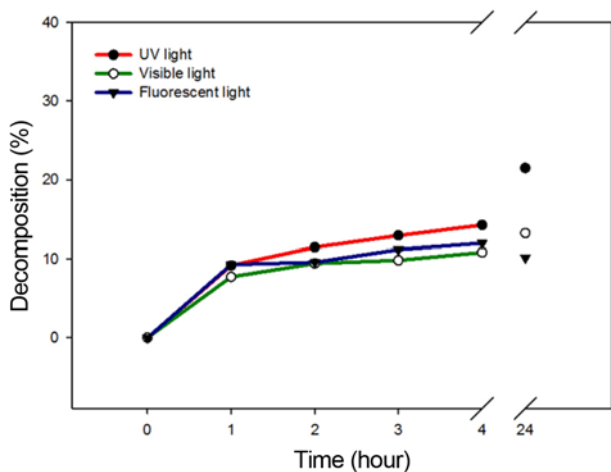


Figure 8. Photocatalytic decomposition rates of the 15 wt% TiO₂/PVA nanofibers contaminated with methylene blue under different light sources.

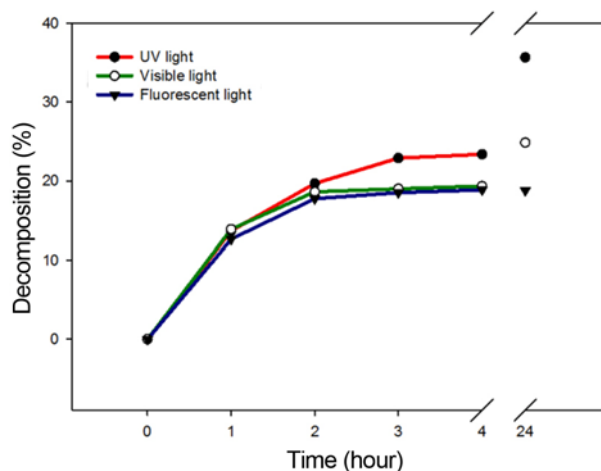


Figure 9. Photocatalytic decomposition rates of the 27 wt% TiO₂/PVA nanofibers contaminated with methylene blue under different light sources.

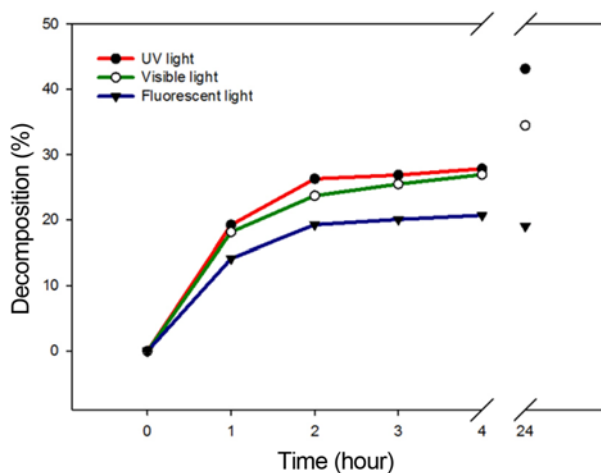


Figure 10. Photocatalytic decomposition rates of the 42 wt% TiO₂/PVA nanofibers contaminated with methylene blue under different light sources.

even though the fraction of UV light in indoor illumination is considerably smaller than that observed in sunlight, some organic compounds and microorganisms can also be decomposed on the TiO₂ surface under weak UV illumination. Previous studies [4,23] exhibited the photocatalytic disinfection of bacteria by TiO₂ catalyst under fluorescent light. Wei *et al.* [24] also demonstrated the bactericidal activity of TiO₂ photocatalysts in aqueous media under UV-visible light having wavelengths of more than 380 nm. Our observations indicate that, besides bactericidal activities, self-cleaning photocatalytic activities were feasible on the TiO₂/PVA nanocomposite fiber webs in the presence of fluorescent and visible light.

To assess the self-cleaning effects against organic dirt in real-life situations, the PVA/TiO₂ nanocomposite fiber webs

were contaminated by red wine. Their photocatalytic self-cleaning properties were assessed under different lighting conditions. As depicted in Figure 11, the decomposition rates of the red wine stains gradually increased with the time of UV light exposure at all the investigated TiO_2 concentrations. After UV irradiation for 24 h, the decomposition rates of the red wine stains were 35.5 %, 45.7 %, and 45.7 %, respectively, for the fiber webs containing 15, 27, and 42 wt% TiO_2 nanoparticles. The fibers containing 27 and 42 wt% TiO_2 nanoparticles, thus, exhibited almost similar decomposition rates after 24 h of UV irradiation. Interestingly, the pristine PVA fiber webs exhibited some degree of photodegradation of the red wine stains, which was different from the negligible degradation effect in case of methylene blue stains. The chromophore(s) of the red

wine may be partially decomposed by photo-oxidation under UV irradiation without any photocatalytic reactions.

Decomposition of the red wine stains was further examined under visible and fluorescent light. Figures 12-14 illustrate their decomposition rates by the composite fiber webs containing 15, 27, and 42 wt% TiO_2 nanoparticles under different light sources. Similarly, the decomposition rates of the red wine stains by the TiO_2 -loaded nanofiber webs also followed the order of fluorescent light < visible light < UV light. Besides, the composite fibers containing 27 and 42 wt% TiO_2 nanoparticles also exhibited similar decomposition rates after being irradiated by visible or fluorescent light for 24 h. Excess TiO_2 loading, thus, did not enhance the self-cleaning photocatalytic effect for red wine stains once an appropriate level of TiO_2 loading was achieved.

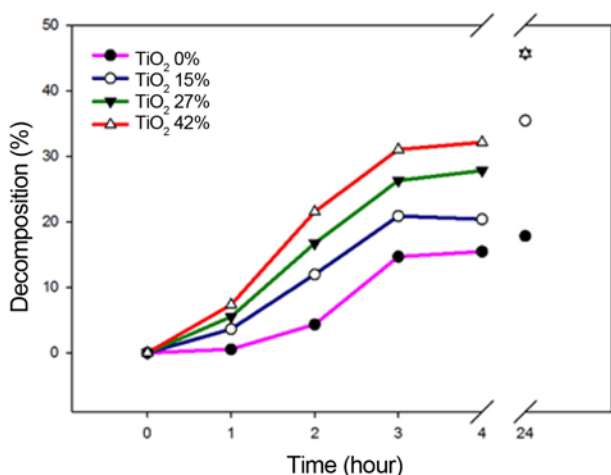


Figure 11. Degradation of the red wine stains on the TiO_2 nanocomposite fibers as a function of UV irradiation time.

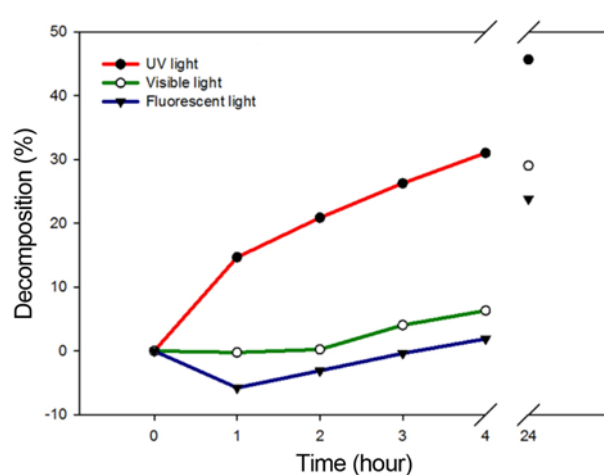


Figure 13. Photocatalytic decomposition rates of the 27 wt% TiO_2 /PVA nanofibers contaminated with red wine under different light sources.

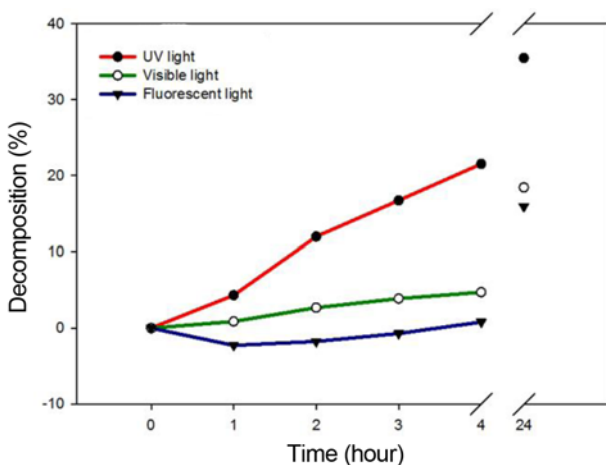


Figure 12. Photocatalytic decomposition rates of the 15 wt% TiO_2 /PVA nanofibers contaminated with red wine under different light sources.

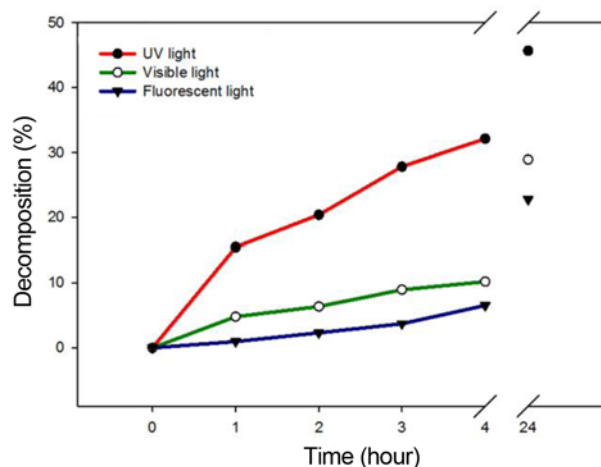


Figure 14. Photocatalytic decomposition rates of the 42 wt% TiO_2 /PVA nanofibers contaminated with red wine under different light sources.

Our observations indicate that TiO₂/PVA composite nanofibers that contain 42 wt% TiO₂ nanoparticles exhibited the self-cleaning photocatalytic effect to the largest extent for methylene blue stains within the tested TiO₂ concentration ranges. For red wine stains, composite fibers containing 27 wt% TiO₂ nanoparticles had similar decomposition rates as those containing 42 wt% TiO₂. Based on these observations, TiO₂ concentrations of 27-42 wt% are assumed to be optimum for the self-cleaning function of the TiO₂/PVA composite nanofibers. However, the physical properties of the composite fibers with high TiO₂ content need to be examined to see if adding too many nanoparticles has any adverse effect on the mechanical properties of the fibers.

Our findings demonstrated the self-cleaning performance of the electrospun composite fibers containing TiO₂ nanoparticles not only under UV light but also under visible and fluorescent light that are commonly used indoors. From a practical viewpoint for future applications of self-cleaning fibrous materials, the self-cleaning activity of the composite fibers under typical indoor lights as well as sunlight is important. Our observations indicate that the photocatalytic activities under visible light or fluorescent light were lower than those under UV light. Therefore, further research is required to increase the efficiency of photocatalysts in indoor lighting conditions. It has been reported that the electrospun composite fibers containing TiO₂ nanoparticles possessed outstanding antimicrobial and UV-protective properties as well as pollutant-decomposing properties [25]. This study adds value to the multifunctionality of the TiO₂ nanocomposite fibers, which may broaden their potential applications.

Conclusion

With increased interest in environmental issues, self-cleaning materials, which are labor saving and eco-friendly, have gained considerable attention. In this study, TiO₂ nanoparticles were incorporated into PVA nanofibrous structures via electrospinning. The composite fiber webs containing varied amounts of TiO₂ were investigated as a photocatalytic self-cleaning system under different light sources.

Bead-free and uniform composite fibers containing 15, 27, and 42 wt% TiO₂ nanoparticles (on a dry basis) were successfully fabricated. The fiber diameters ranged from 180 to 250 nm. TEM and EDX analysis of the composite fibers confirmed the presence of TiO₂ in the fibers. The heat treatment conditions were identified for stabilizing the TiO₂/PVA nanocomposite fibers containing varied amounts of TiO₂ nanoparticles in an aqueous environment. The TiO₂/PVA nanocomposite fiber webs exhibited photocatalytic decomposition of the methylene blue and red wine stains under visible and fluorescent light as well as UV irradiation. Generally, the decomposition rate increased by increasing

the time of light exposure and the TiO₂ concentration.

This study revealed that the organic contaminants are decomposed by the TiO₂ nanocomposite fibers not only under UV light but also under visible light and fluorescent light, which illuminated the possibility of using the self-cleaning activity of the TiO₂ nanocomposite fibers in both indoor and outdoor environments. The TiO₂ nanocomposite fibers not only possess self-cleaning properties but also possess antimicrobial, pollutant-decomposing, and UV-protective properties. Therefore, it would be useful to destroy harmful bacteria and perform self-cleaning by the simultaneous photocatalytic action of the TiO₂-loaded nanofibers. The TiO₂ nanocomposite fibers containing multiple functionalities exhibit high potential for usage in various applications, including outdoor textiles, such as work clothing and sportswear, as well as indoor textile products, such as medical and interior textiles.

Acknowledgements

This research was supported by the Basic Science Research Program through the National Research Foundation of Korea (NRF) funded by the Ministry of Education, Science and Technology (NRF-2010-0013511); and the Brain Korea 21 Plus Project of Dept. of Clothing and Textiles, Yonsei University in 2018.

References

1. I. P. Parkin and R. G. Palgrave, *J. Mater. Chem.*, **15**, 1689 (2005).
2. A. Fujishima and X. Zhang, *C. R. Chimie.*, **9**, 750 (2006).
3. W. S. Tung and W. A. Daoud, *J. Mater. Chem.*, **21**, 7858 (2011).
4. A. Pal, S. O. Pehkonen, L. E. Yu, and M. B. Ray, *J. Photochem. Photobiol. A*, **186**, 335 (2007).
5. M. R. Hoffmann, S. T. Martin, W. Choi, and D. W. Behnemann, *Chem. Rev.*, **95**, 69 (1995).
6. H. D. Jang, S. K. Kim, and S. J. Kim, *J. Nanopart. Res.*, **3**, 141 (2001).
7. N. S. Allen, N. Mahdjoub, V. Vishnyakov, P. J. Kelly, and R. J. Kriek, *Polym. Degrad. Stabil.*, **150**, 31 (2018).
8. J. Wang, J. Zhao, L. Sun, and X. Wang, *Text. Res. J.*, **85**, 1104 (2015).
9. R. Benedix, F. Dehn, J. Quaas, and M. Orgass, *Lacer*, **5**, 157 (2000).
10. W. A. Daoud and J. H. Xin, *J. Am. Ceram. Soc.*, **87**, 953 (2004).
11. K. Qi, X. Wang, and J. H. Xin, *Text. Res. J.*, **81**, 101 (2011).
12. A. Bozzi, T. Yuranova, and J. Kiwi, *J. Photochem. Photobiol. A*, **172**, 27 (2005).
13. M. I. Mejia, J. M. Marin, G. Restrepo, C. Pulgarin, E. Mielczarski, J. Mielczarski, Y. Arroyo, J.-C. Lavanchy,

- and J. Kiwi, *Appl. Catal. B-Environ.*, **91**, 481 (2009).
14. K. T. Meilert, D. Laub, and J. Kiwi, *J. Mol. Catal. A: Chem.*, **237**, 101 (2005).
 15. Z. Liuxue, W. Xiulian, L. Peng, and S. Zhixing, *Surf. Coat. Tech.*, **201**, 7607 (2007).
 16. N. Veronovski, A. Rudolf, M. S. Smole, T. Kreže, and J. Geršak, *Fiber. Polym.*, **10**, 551 (2009).
 17. A. Greiner and J. H. Wendorff, *Angew. Chem. Int. Ed.*, **46**, 5670 (2007).
 18. J. W. Yoon, Y. Park, J. Kim, and C. H. Park, *Fash. Text.*, **4**, 9 (2017).
 19. J. Zeng, J. Sun, H. Hou, R. Dersch, H. Wickel, J. H. Wendorff, and A. Greiner in "Polymeric Nanofibers" (D. H. Reneker and H. Fong Eds.), pp.163-172, American Chemical Society, Oxford University Press, Washington, DC, 2006.
 20. N. M. Bedford and A. J. Steckl, *ACS Appl. Mater. Inter.*, **2**, 2448 (2010).
 21. C. J. Hurren, R. T. Liu, X. Liu, and X. G. Wang in "Advances in Science and Technology" (P. Vincenzini and R. Paradiso Eds.), Vol. 60, pp.111-116, Trans Tech Publications, 2008.
 22. H. J. Lee, J. Kim, and C. H. Park, *Text. Res. J.*, **84**, 267 (2014).
 23. L. Caballero, K. A. Whitehead, N. S. Allen, and J. Verran, *J. Photochem. Photobiol. A*, **202**, 92 (2009).
 24. C. Wei, W. Y. Lin, Z. Zainal, N. E. Williams, K. Zhu, A. P. Kruzic, R. L. Smith, and K. Rajeshwar, *Environ. Sci. Technol.*, **28**, 934 (1994).
 25. K. Lee and S. Lee, *J. Appl. Polym. Sci.*, **124**, 4038 (2012).